Regulation of Synovial γδ T Cell Ligand Expression by Mitochondrial Reactive Oxygen Species and Gasdermin-D

Cheryl C. Collins,* Peter Hahn,* Zhaozhao Jiang,† Katherine A. Fitzgerald,† Tsan Sam Xiao,‡ and Ralph C. Budd*

γδ T cells reside at mucosal and epithelial barriers, and they often accumulate at sites of inflammation, both infectious and autoimmune, as well as in certain tumors. However, progress in understanding their function is considerably hampered by a lack of full understanding of the ligands recognized by TCR-γδ and how expression of these ligands is regulated. We recently developed a soluble human TCR-γδ (Vγ9Vδ1) tetramer from a synovial γδ T cell clone of a Lyme arthritis patient and observed that it stains monocytes activated by *Borrelia burgdorferi*. Those findings are extended in the current study to further examine the physiological regulation of ligand expression on monocytes. The TCR-γδ ligand is induced by a variety of TLR agonists and requires NF-κB activation. Of particular interest is that ligand expression also requires caspase activation of the inflammasome and is dependent on active metabolism, mitochondrial reactive oxygen species, and activation of gasdermin-D. Consistent with these observations, the TCR-γδ ligand is expressed by a subset of metabolically active $CD14^+CD16^+$ monocytes and colocalizes intracellularly with mitochondria. The findings suggest a model in which synovial γδ T cell ligand is a self-antigen whose surface expression is increased by inflammatory conditions and mitochondrial stress. *The Journal of Immunology*, 2023, 210: 61–71.

γδ T cells remain something of an enigma in immunology. They arose with the earliest appearances of T and B lymphocytes of the adaptive immune system and have been maintained as a "third rail" since then throughout all vertebrate species (1–3). This may speak to their nonredundant function in the immune system. γδ T cells have demonstrated their importance in the immune response to numerous infections (4–10), cancer (11, 12), and autoimmunity (13–20). They also function in tissue repair and homeostasis, as evidenced by their role in skin wound healing and thermogenesis (21–24). Despite becoming activated during various infections, there is little evidence that TCR-γδ cells directly recognize foreign microbial Ags (25). In addition, γδ T cell activation is not restricted by classical MHC molecules (26). Rather, there is growing evidence that γδ T cells respond to self-ligands that are upregulated during infection, cancer, or autoimmunity, potentially by a common mechanism of cell stress or death (2).

Of the various γδ T cell ligands that have been proposed, there is general agreement that these include various self-proteins, sometimes in the presence of nonprotein components (27–30). Currently there is no apparent common structural motif for the proposed TCR-γδ ligands, apart from nonclassical MHC-like molecules such as CD1 and butyrophilins (27–30). But even recognition of these molecules may involve additional components, such as sulfatide in the case of CD1d (29), or phosphoantigens in the case of butyrophilins (27, 28). This lack of full understanding of TCR-γδ ligands and their physiological regulation leaves a considerable gap in our comprehension of the biology of γδ T cells.

We recently reported the development of a human soluble TCR-γδ (sTCR-γδ) tetramer derived from a synovial γδ T cell clone of a Lyme arthritis patient (31). The original γδ T cell clone is stimulated by *Borrelia burgdorferi* in the presence of human monocytes but does not activate in response to *Borrelia* alone (32). In agreement with this, stimulation of monocytes with *Borrelia* induced significant surface expression of ligand (31). Ligand expression was sensitive to trypsin digestion, attesting to the protein nature of the ligand. The current studies extend these findings through an examination of the physiological regulation of ligand expression. Because *Borrelia* lipopeptides stimulate monocytes through TLR2 (33), we hypothesized that *Borrelia* and other TLR ligands would induce TCR-γδ ligands via TLR-mediated signal pathways and involve the inflammasome and metabolic stress. We observe that ligand is induced on monocytes by a variety of TLR ligands and is blocked by inhibition of the NF-κB pathway, as well as inhibitors of the inflammasome and gasdermin-D activation. Ligand expression is also regulated by mitochondrial reactive oxygen species (ROS), which were recently shown to promote gasdermin-D activation (34, 35). Collectively, the

*Department of Medicine, Vermont Center for Immunology and Infectious Diseases, Larner College of Medicine, The University of Vermont, Burlington, VT; †Department of Medicine, University of Massachusetts Medical School, Worcester, MA; and ‡Department of Pathology, Case Western Reserve University, Cleveland, OH

ORCIDs: 0000-0003-2608-4161 (P.H.); 0000-0002-9768-8491 (Z.J.); 0000-0001-9688-475X (T.S.X.); 0000-0001-8524-8758 (R.C.B.).

Received for publication December 13, 2021. Accepted for publication November 1, 2022.

This work was supported by National Institute of Allergy and Infectious Diseases Grants AI107298 and AI119979 (to R.C.B.) and National Institute of General Medical Sciences Grants GM118228 (to R.C.B.) and GM127609 (to T.S.X). The Cytek Aurora support is from the National Institutes of Health Grant S10-ODO026843.

C.C.C. developed the sTCR-γδ vector and its insertion into the baculovirus vector, production of sTCR-γδ tetramers, purification of PBMCs and monocytes, and performed a portion of the flow cytometry and confocal microscopy; P.H. performed some of the flow cytometry analysis and contributed to figure preparation; Z.J., K.A.F., and T.S.X. assisted with studies of gasdermin-D inhibition and manuscript preparation; and R.C.B. supervised all experiments and wrote the manuscript.

Address correspondence and reprint requests to Dr. Ralph C. Budd, The University of Vermont Larner College of Medicine, Given Medical Building D-305, 89 Beaumont Avenue, Burlington, VT 05405. E-mail address: ralph.budd@med.uvm.edu

The online version of this article contains supplemental material.

Abbreviations used in this article: Hsp, heat shock protein; MLKL, mixed lineage kinase domain-like protein; NLRP3, NOD-like receptor family pyrin domain containing 3; poly(I:C), polyinosinic-polycytidylic acid; ROS, reactive oxygen species; RT, room temperature; sTCR-γδ, soluble TCR-γδ; TRAF6, TNFR-associated factor 6; TRIF, Toll/IL-1R domain-containing adapter inducing IFN-β.

findings are consistent with the role of γδ T cells in the immune surveillance of cell stress and inflammation.

Materials and Methods

Production of sTCR-γδ

Human synovial γδ T cell clones from a Lyme arthritis patient were produced as previously described (14, 25). One of these clones, Bb15 (Vγ9Vδ1), was chosen for production of the sTCR-γδ using modification of a previously reported procedure (36, 37). Both TCR chains were produced as a single transcript in a baculovirus vector. The pBACp10pH vector used contains two back-to-back promoters, p10 and polyhedrin. The p10 promoter is followed by multiple cloning sites for the γ-chain, and the polyhedrin promoter is followed by multiple cloning sites for the δ-chain. Downstream of the γ-chain we placed a hexa-His tag for nickel column purification, followed by a biotinylation sequence for tetramerization. The γ-chain and δ-chain were PCR amplified using high-fidelity polymerase (Deep Vent polymerase, New England Biolabs). Both TCR chain sequences were verified following the initial PCR amplification as well as after insertion into the pBACp10pH vector. Virus encoding the sTCR-γδ was generated by cotransfection of Sf21 moth cells using the Sapphire baculovirus DNA and transfection kit (Orbigen) with the sTCR pBACp10pH construct. Virus was harvested 6 d later and used as primary (P1) stocks. Two additional rounds of viral amplification, P2 and P3, were completed using midlog phase Sf21 cells (~1.6×10^6 cells/ml) allowed to adhere for 1 h before infecting at a multiplicity of infection of 0.01 or 0.1 with P1 and P2 stocks, respectively. After 72 h of infection, culture media were clarified by centrifugation (1000 × *g* for 10 min) and filtration (VacuCap 90PF 0.8/0.2-μm Supor membrane filter units; Pall, Westborough, MA) before storing in the dark at 4°C until use. Protein production occurred in 12-l batches of midlog phase (~1.6×10^6 cells/ml) Hi5 cells growing in suspension (0.5 l of culture in 1-l spinner flasks) and infected with P3 stock at a 1:50 dilution. Following 72 h of infection, cells were removed by centrifugation and filtration as described above. The filtered supernatant (~12 l) containing secreted sTCR-γδ was concentrated to ~100 ml before dialyzing against 1 l of nickel column loading buffer (20 mM sodium phosphate buffer [pH 7.4], 20 mM imidazole, 0.5 M NaCl) using a Pellicon diafiltration system with two 10-kDa molecular mass cutoff membranes (Millipore, Burlington, MA) back down to ~100 ml. After system flushing, the final sample volume was ~200 ml. It was then loaded onto loading buffer–equilibrated His-Trap HP columns (GE Healthcare, Little Chalfont, U.K.) at 100 ml per 2.5-ml column. Columns were washed with at least 10 column volumes of loading buffer until baseline absorption was achieved. Bound proteins were eluted using a gradient from 20 to 500 mM imidazole over 20 column volumes. Elution was monitored by absorbance at 280 nM, and 1-ml fractions were collected. Fractions containing the target protein were identified using SDS-PAGE gel analysis using Coomassie Blue. High purity (>95%) sTCR-γδ fractions were pooled, dialyzed against PBS (pH 7.4), and frozen at −80°C until used in future studies. Yields were typically ~1.0–2.5 mg/l culture. Purified sTCR-γδ was then biotinylated using a biotin-protein ligase system (Avidity Biosciences) and tetramerized with streptavidin-PE (BioLegend) for FACS staining. Verification of TCR-γδ protein was confirmed by SDS-PAGE gel analysis using Coomassie Blue as well as immunoblot using Abs to Vδ1 or Cγ (Endogen) (14, 25).

Purification and activation of human monocytes

Human PBMCs were obtained using an approved protocol from the University of Vermont Human Studies Committee. Monocytes were purified from PBMCs using CD14-labeled magnetic beads, followed by column purification (Miltenyi Biotec), and then cultured in RPMI 1640 complete with 5% bovine calf serum in the absence or presence of either a *B. burgdorferi* sonicate (10 μg/ml), LPS (10 ng/ml) (InvivoGen), polyinosinic-polycytidylic acid (poly(I:C); 5.0 μg/ml) (InvivoGen), or CpG (2.5 μM) (InvivoGen) for 24 or 48 h. A variety of inhibitors were added to some of these cultures. These include the TBK1 inhibitor GSK8612 (10 μM) (Selleckchem), TNFR-associated factor 6 (TRAF6) inhibitor 6877002 (10 μM) (Tocris/Bio-Techne), Toll/IL-1R domain-containing adapter inducing IFN-β (TRIF) inhibitor resatorvid (10 nM) (MedChemExpress), IKK inhibitor BMS-345541 (1 μM) (MilliporeSigma Calbiochem), RIPK1 inhibitor necrostatin (50 μM) (R&D Systems), NOD-like receptor family pyrin domain containing 3 (NLRP3) inhibitor MCC950 (3 μM) (MilliporeSigma), caspase-1 inhibitor YVAD-CMK (40 μM)

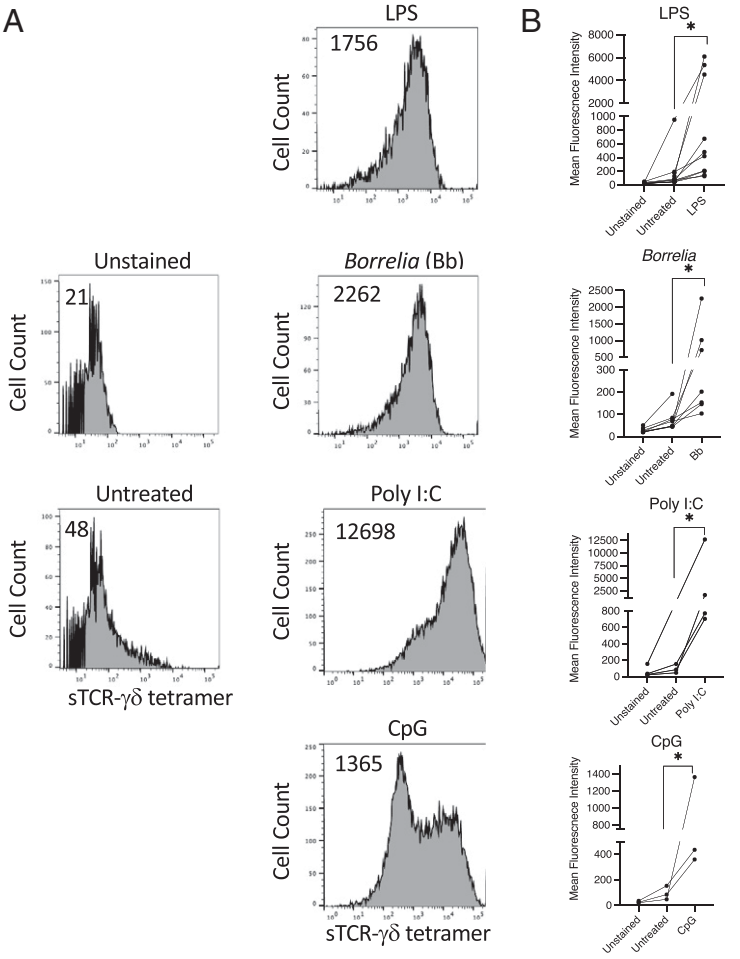

FIGURE 1. TLR agonists induce TCR-γδ ligand surface expression on monocytes. Freshly isolated human monocytes were untreated or activated with LPS (10 ng/ml) *B. burgdorferi* (Bb) (10 μg/ml), poly(I:C) (5.0 μg/ml), or CpG (2.5 μM) for 48 h, then stained with sTCR-γδ tetramer-PE (10 μg/ml). (**A**) Representative histograms with number inserts indicating mean fluorescence intensity of entire histogram. (**B**) Graphs summarize findings from all experiments. *$p < 0.05$.

(Sigma-Aldrich), caspase-3 inhibitor DEVD-FMK (20 μM) (R&D Systems), caspase-8 inhibitor IETD-FMK (20 μM) (R&D Systems), pan-caspase inhibitor zVAD-FMK (20 μM) (MP Biomedicals), mitochondrial antioxidant MitoQ (10 and 100 μM) (MitoQ), glucose competitive inhibitor 2-deoxyglucose (5 mM) (Sigma), inhibitor of carnitine palmitoyltransferase 1a and fatty acid oxidation etomoxir (200 μM) (Tocris/Bio-Techne), and a variety of inhibitors of gasdermin-D, including FLTD (100 μM), necrosulfonamide (10 μM) (MilliporeSigma Calbiochem), dimethyl fumarate (25 μM) (Sigma-Aldrich), and fumarate hydratase inhibitor FHIN1 (25 μM) (MilliporeSigma/MedChemExpress),

Flow cytometry

Cells were stained with sTCR-γδ–PE tetramer (10 μg/ml), CD14-allophycocyanin (BioLegend), and CD16 BV421 (BioLegend), anti–heat shock protein (Hsp)70-PE (Miltenyi Biotec), or anti–annexin A2-PE (Cell Signaling Technology), and samples were run on a MACSQuant VYB (Miltenyi Biotec) or Cytek Aurora. Analysis was confined to living cells based on Live/Dead staining (BD Biosciences).

Cytokine detection by Luminex assay

Cytokine levels of IL-1β were detected using a Luminex immunoassay (R&D Systems) according to the manufacturer's protocol. Briefly, samples were analyzed undiluted or diluted 1:2 in RPMI 1640 complete media. Then, 50 μl of the magnetic bead working solution was added to each well, after which 50 μl of appropriate samples or standards were added to wells and incubated at room temperature (RT) for 120 min at 800 rpm on an IKA MS 3 digital shaker. After three washes with 100 μl of Luminex wash buffer, 50 μl of the biotin detection beads was added to each well and incubated for 60 min at RT at 800 rpm. Following another set of three washes, 50 μl of streptavidin-PE in wash buffer was added to each well and incubated for 30 min at RT at 800 rpm. After an additional three washes, 100 μl of wash buffer was added to each well and shaken for 1 min at 800 rpm. Sample data were read and analyzed with Bio-Plex Manager software.

Confocal microscopy

Purified monocytes were washed in prewarmed RPMI 1640 without phenol red in 5-mm polystyrene tubes. Cells were then stained with LysoView 488 (1:4000) (Biotium, Fremont, CA, no. 70067) for 30 min, MitoTracker Deep Red FM (Molecular Probes/Invitrogen, no. M22426) (50 nM) for 45 min, and sTCR-γδ–PE (10 μg/ml) or negative control IgG-PE (10 μg/ml) for 60 min. All incubations were at 37°C and 5% CO_2. Cells were again washed in prewarmed RPMI 1640, then stained with Hoechst 33342 nuclear stain (Fisher Scientific, no. 62249) for 10 min at RT. After one final wash, cells were resuspended in 150 μl of prewarmed RPMI 1640, transferred onto glass-bottom microwell dishes (MatTek, Ashland, MA), and allowed to adhere for 20–30 min.

Monocytes were imaged in a Tokai Hit stage top incubator (model INUBG2A-TIZB) attached to a Nikon A1R HD laser scanning confocal microscope (Nikon Instruments, Melville, NY) utilizing a ×40 Plan Fluor (numerical aperture 1.3, working distance 0.24) objective lens. Image scan zoom was set to 2.0, accomplishing 0.15 μm per pixel image resolution and imaged via a galvanometric scanner. Cells were imaged using 405-, 488-, 561-, and 640-nm lasers and collected with 450/50-, 525/50-, 600/50-, and 685/70-nm bandpass filters, respectively. Laser power and gain settings were established by imaging an unstained control sample. Imaging parameters remained constant for all images acquired within the dataset. Z stacks were acquired with sequential scanning over ~30 μm in depth with a step interval of 0.625 μm. Images were saved in the ND2 file format in NIS Elements (version 5.2.1, Nikon, Tokyo, Japan).

Colocalization analysis

Z stacks of images were analyzed for fluorophore colocalization using Volocity version 6.3.0 (PerkinElmer, Waltham, MA). Images were opened in the colocalization tab, and cells that were completely contained within the image boundary were circled with the ROI (region of interest) tool. A scatterplot of the channels to be analyzed was used to manually threshold the image to exclude background fluorescence. Background levels for PE staining and MitoTracker Deep Red staining were set based on the background levels observed in an unstained monocyte sample. The LysoView 488 threshold was set so that only distinct punctate lysosomal structure staining was counted. Once the appropriate threshold was determined colocalization was calculated. M1 and M2 values for each cell were reported for the relationship between LysoView 488 and sTCR-γδ–PE staining, as well as the relationship between MitoTracker Deep Red and sTCR-γδ–PE staining. This process was repeated for all healthy cells contained within the image boundary. A total of 67 cells were measured for colocalization analysis.

Statistical analysis

All experiments were performed at least three times. The following statistical tests were used: paired Student *t* test when comparing two conditions within the same experiment, and one-way ANOVA with a Sidak test for correction for multiple comparisons.

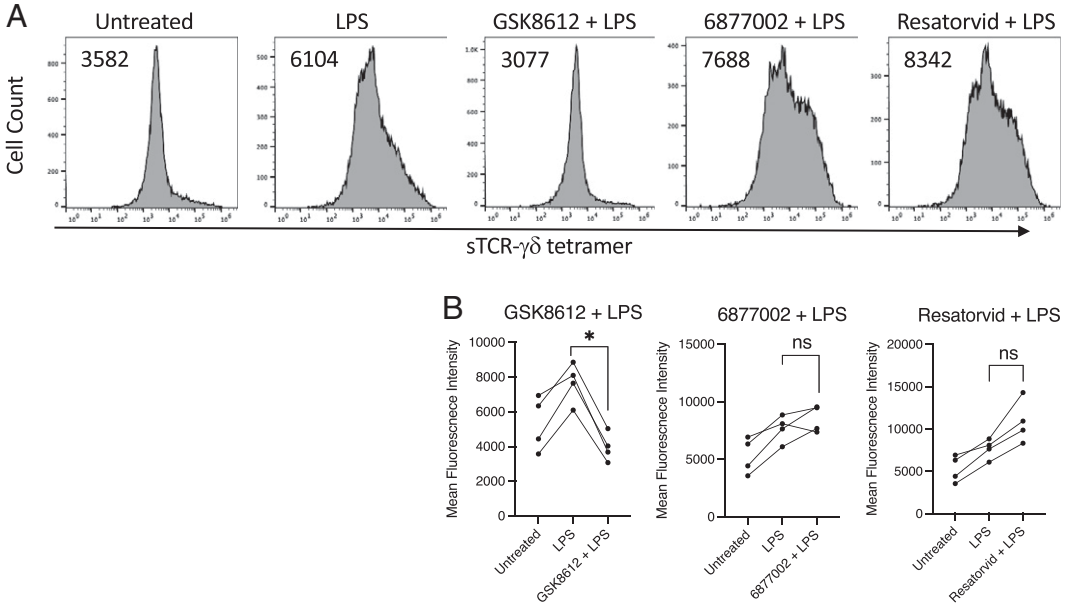

FIGURE 2. LPS-induced TCR-γδ ligand expression is dependent on TBK1. Monocytes were untreated or activated with LPS in the absence or presence of the TBK1 inhibitor GSK8612 (10 μM), the TRAF6 inhibitor 6877002 (10 μM), or the TRIF inhibitor resatorvid (10 μM) for 48 h and then stained with sTCR-γδ tetramer-PE (10 μg/ml). (**A**) Representative histograms with number inserts indicating mean fluorescence intensity of entire histogram. (**B**) Graphs summarize findings from all experiments. *$p < 0.05$. ns, not significant.

Results

Induction of TCR-γδ ligand expression by TLR agonists is NF-κB– and caspase-dependent

We previously observed that our panels of Lyme arthritis synovial γδ T cell clones are activated to produce cytokines by *B. burgdorferi*, a TLR2 agonist, as well as by several other TLR agonists, in the presence of fresh human monocytes (32). We thus initially examined for TCR-γδ ligand expression on TLR-activated monocytes. Whereas untreated monocytes expressed no detectable ligand, activation for 48 h with either *B. burgdorferi*, LPS, poly(I:C), or CpG all induced various levels of sTCR-γδ tetramer staining (Fig. 1).

Because many TLRs stimulate NF-κB and the inflammasome, we examined the effects of inhibitors of these pathways on TCR-γδ ligand expression. Inhibition of TBK1 with GSK8612 completely blocked ligand expression by LPS-activated monocytes, whereas inhibitors of TRAF6 (6877002) and TRIF (resatorvid) had negligible effects (Fig. 2). The NF-κB inhibitor BMS-345541 greatly reduced ligand expression induced by either LPS or *Borrelia* (Fig. 3). LPS stimulation of human monocytes can trigger an "alternative inflammasome" involving TLR-TRIF-RIPK1-FADD-caspase-8 signaling upstream of NLRP3 (38). However, the NLRP3 inhibitor MCC950 had negligible effects on ligand expression (Fig. 3). These findings paralleled the observation that NF-κB inhibition blocked production of IL-1β whereas inhibition of NLRP3 did not (Fig. 3).

The possible contribution of the inflammasome to TCR-γδ ligand expression was examined further by inhibiting specific caspases. Targeting caspase-1 (YVAD) or caspase-8 (IETD) inhibited ligand induction by *Borrelia,* but to a somewhat lesser extent (YVAD) or not at all (IETD) by LPS (Fig. 4). Blocking caspase-3 (DEVD) did not block ligand induction by either *Borrelia* or LPS. However, inhibition of all caspases with the pan-caspase blocker zVAD completely abrogated ligand expression to the level of unstimulated monocytes (Fig. 4). These findings suggested the possibility that several caspases could partly contribute to ligand expression.

TCR-γδ ligand expression is dependent on activation of gasdermin-D

The partial inhibition of ligand expression with caspase-1 blockade suggested the possible involvement of the inflammasome. Activation of the inflammasome can lead not only to pro–IL-1β cleavage, but its export following cleavage and activation of the pore-forming complex gasdermin-D (39). Cleavage of gasdermin-D by caspase-1, caspase-4, or caspase-5 in human cells (caspase-11 in murine cells) releases its N-terminal fragment, which oligomerizes to form a pore complex in the cell membrane (35, 40–42).

Given the ability of zVAD to inhibit all caspases, and to block ligand expression, we more closely examined the potential role of gasdermin-D. Various inhibitors of gasdermin-D activation have been described. Perhaps the most specific inhibitor is the

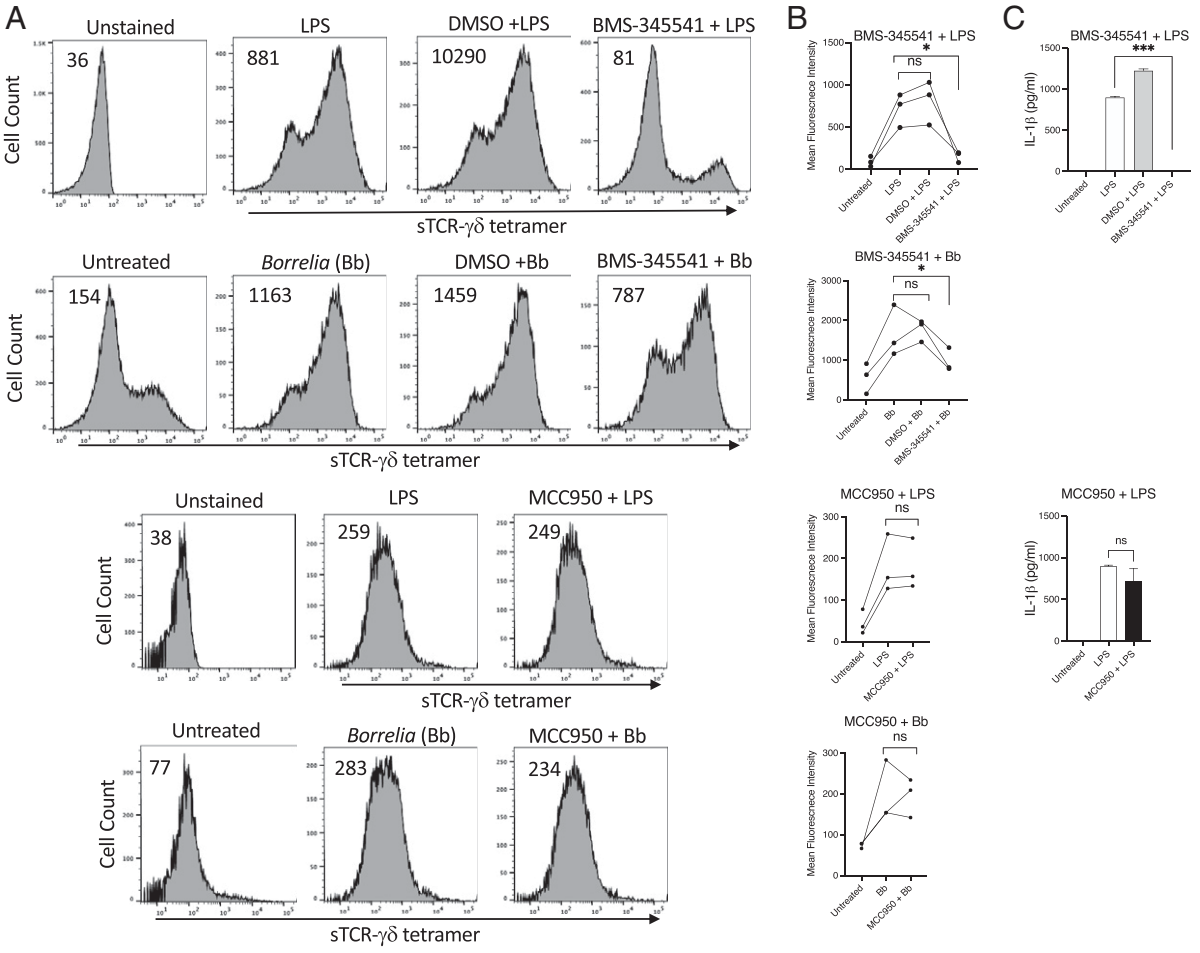

FIGURE 3. NF-κB inhibition blocks expression of TCR-γδ ligand expression. (**A**) Shown are the mean fluorescence intensity of sTCR-γδ tetramer staining of LPS- or *B. burgdorferi* (Bb)–activated monocytes in the absence or presence of DMSO control, the IKK inhibitor BMS-345541 (1 μM), or the NLRP3 inhibitor MCC950 (3 μM). Number inserts indicate mean fluorescence intensity of entire histogram. (**B**) Graphs summarize mean fluorescence intensity from all experiments, and (**C**) IL-1β in culture supernatants. $*p < 0.05$, $***p = 0.0001$. ns, not significant.

tetrapeptide FLTD, which corresponds to the cleavage site in gasdermin-D (43). As shown in Fig. 5, FLTD completely inhibited the expression of TCR-γδ ligand induction by LPS or *Borrelia*. The Krebs cycle intermediate fumarate was recently reported to inhibit gasdermin-D activation through derivatization of a critical Cys^{191}, as well as four additional cysteines, to 2-(succinyl)-cysteine, which inhibited gasdermin-D oligomerization (44). We thus examined the effect of increasing levels of fumarate in LPS- or *Borrelia*-activated monocytes using either dimethyl fumarate to directly increase intracellular fumarate levels, or by inhibiting fumarate metabolism by blocking fumarate hydratase with FHIN1 (44). Both agents greatly reduced surface expression of the TCR-γδ ligand (Fig. 5). Necrosulfonamide also inhibits gasdermin-D activation through alkylating the same cysteine residue Cys^{191} (45). Necrosulfonamide also strongly blocked surface ligand expression (Fig. 5). Collectively, the findings support the view that TCR-γδ ligand expression by activated monocytes requires activation of gasdermin-D. Similar results were observed with the inhibitors following activation with poly(I:C) or CpG (Supplemental Figs. 1, 2).

Necrosulfonamide has been reported to also inhibit pore formation by mixed lineage kinase domain-like protein (MLKL) (46), which is activated by RIPK1–RIPK3. To thus assess the possible contribution of MLKL in ligand expression we inhibited MLKL pore formation of the necroptosome with the RIPK1 inhibitor necrostatin (47). However, necrostatin only modestly reduced ligand expression by *Borrelia* and not at all with LPS (Fig. 6).

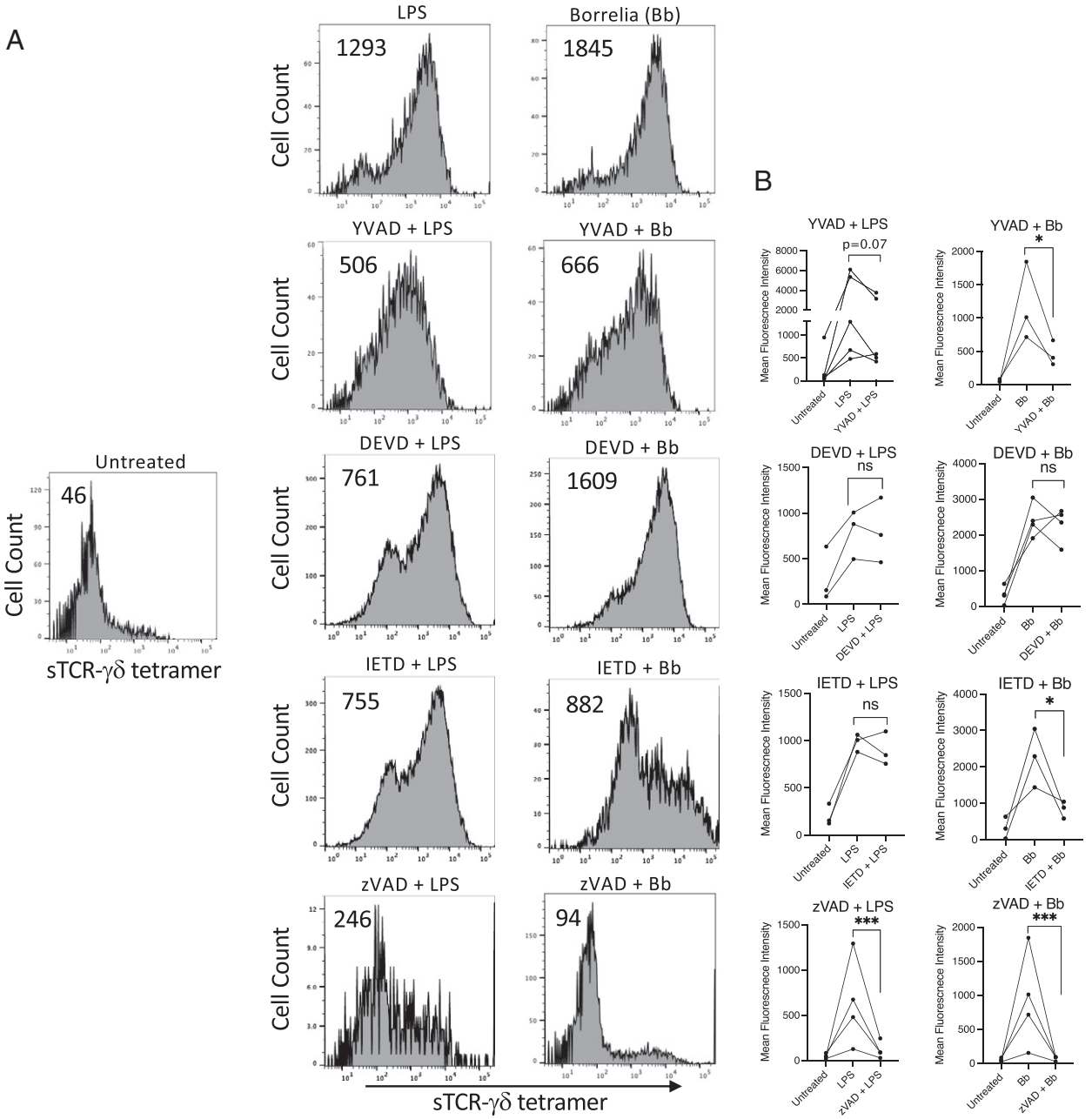

FIGURE 4. TCR-γδ ligand expression is reduced by inhibiting caspases. Monocytes were activated with LPS of *B. burgdorferi* (Bb) in the absence or presence of inhibitors of caspase-1 (YVAD) (40 μM), caspase-3 (DEVD) (20 μM), caspase-8 (IETD) (20 μM), or the pan-caspase inhibitor zVAD (20 μM). (**A**) Representative histogram with number inserts indicating mean fluorescence intensity of entire histogram. (**B**) Graphs summarize findings from all experiments. $*p < 0.05$, $***p < 0.0005$. ns, not significant.

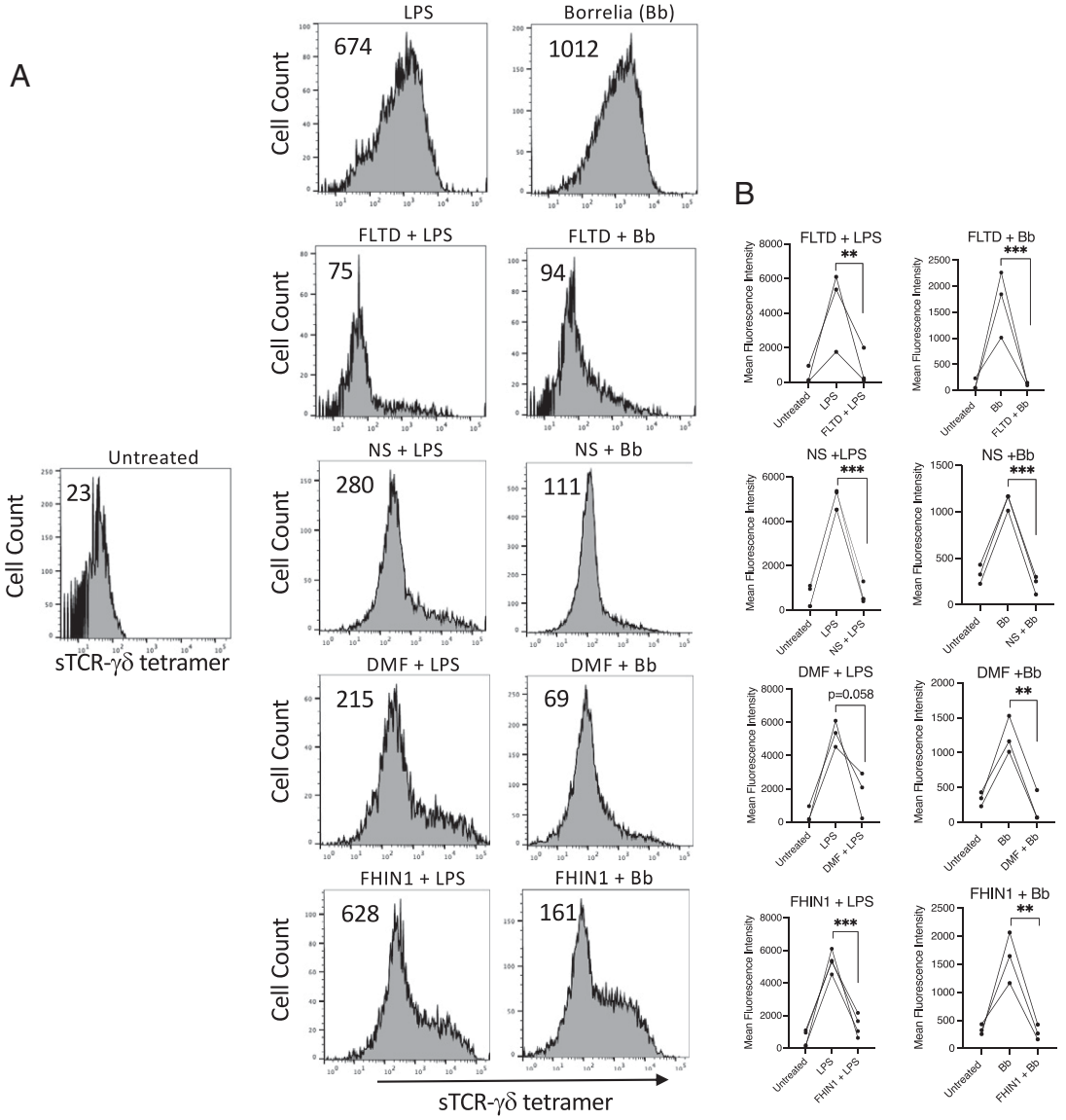

FIGURE 5. Gasdermin-D activation is required for surface expression of TCR-γδ ligand. LPS- or *B. burgdorferi* (Bb)–activated monocytes were treated with either FLTD (100 μM), necrosulfonamide (NS) (10 μM), dimethyl fumarate (DMF) (25 μM), or fumarate hydratase inhibitor FHIN1 (25 μM). After 48 h cells were stained with sTCR-γδ tetramer. (**A**) Representative histograms with number inserts indicating mean fluorescence intensity of entire histogram. (**B**) Graphs summarize findings from all experiments. $^{**}p < 0.005$, $^{***}p < 0.0005$.

TCR-γδ ligand expression is driven by metabolic and redox state of activated monocytes

LPS is known to induce ROS in monocytes and dendritic cells (48, 49). In addition, mitochondrial ROS were recently reported to promote oligomerization and activation of gasdermin-D (35). We therefore blocked mitochondrial ROS using the mitochondrially targeted antioxidant MitoQ (50–52). MitoQ efficiently blocked both surface TCR-γδ ligand expression and lL-1β production in a dose-dependent manner (Fig. 7). LPS also promotes robust metabolic changes in monocytes, including activation of fatty acid oxidation and glycolysis. These alterations were inhibited using either etomoxir, an inhibitor of carnitine palmitoyltransferase-1 and fatty acid uptake (53, 54), or 2-deoxyglucose, a competitive inhibitor of glucose utilization (55). Both agents extensively blocked TCR-γδ ligand expression (Fig. 7).

TCR-γδ ligand expression by a subset of metabolically active $CD14^+$ $CD16^+$ monocytes

Freshly isolated human monocytes can be subset according to the expression of CD14 (LPS coreceptor) and CD16 (FcγRIII) into $CD14^+CD16^-$ classical monocytes and $CD14^+CD16^+$ inflammatory monocytes, with the latter expressing high levels of inflammatory cytokines, including IL-1β, higher Ag-presenting potential, and greater metabolic activity (56). $CD14^+CD16^+$ monocytes are believed to derive from the $CD14^+CD16^-$ subset following in vivo activation, and their numbers are increased in various infections (56–58). Based on our in vitro activation studies and the observation that a small subpopulation of untreated total monocytes frequently expressed TCR-γδ ligand (see Fig. 3, untreated), we examined ligand expression on subsets of freshly isolated monocytes and observed that the $CD14^+CD16^+$ subset expressed considerably higher levels of the TCR-γδ ligand than did other subsets (Fig. 8).

Intracellular TCR-γδ ligand expression colocalizes with mitochondria

Given that surface TCR-γδ ligand is expressed by metabolically active monocytes and requires gasdermin-D pore formation to reach the cell surface, we considered that ligand might be present intracellularly and that it might localize with sites of metabolic activity. We

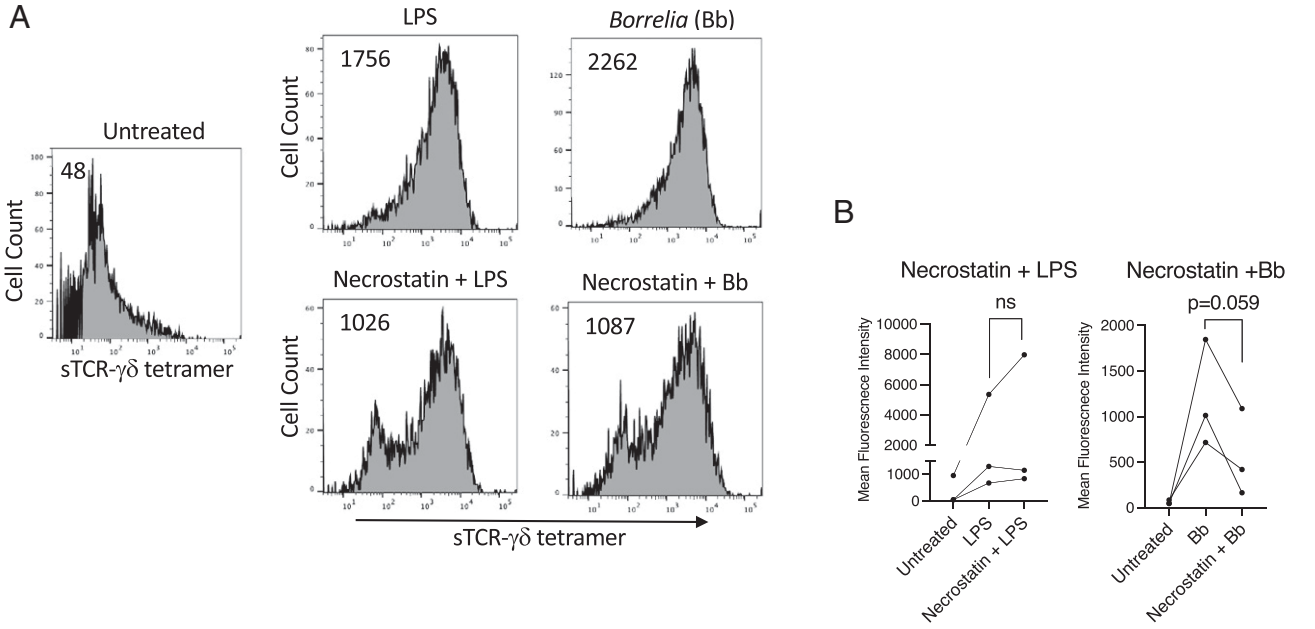

FIGURE 6. TCR-γδ ligand expression is only minimally inhibited by blocking necroptosis. LPS- or *B. burgdorferi* (Bb)–activated monocytes were either untreated or treated with the RIPK1 inhibitor necrostatin (50 μM). After 48 h cells were stained with sTCR-γδ tetramer. (**A**) Representative histograms with number inserts indicating mean fluorescence intensity of entire histogram. (**B**) Graphs summarize findings from all experiments. ns, not significant.

thus performed confocal microscopic analysis of freshly isolated monocytes stained with TCR-γδ tetramer, LysoView to identify lysosomes, MitoTracker to identify mitochondria, and Hoechst staining of nuclei. As shown in Fig. 9, nearly all TCR-γδ tetramer staining colocalized with mitochondria (colocalization coefficient = 0.723), whereas only a small proportion colocalized with lysosomes (colocalization coefficient = 0.128).

Discussion

In this study, we demonstrate that the ligand for a human synovial Vγ9Vδ1 T cell is induced in vitro by monocytes activated by various TLR ligands, and it is also expressed on a naturally occurring $CD14^+$ $CD16^+$ subset of fresh monocytes that is known to be metabolically active (56–58). Consistent with TLR activation of the NF-κB and inflammasome/gasdermin-D pathways, ligand expression was also dependent on these pathways. Additionally, the current findings reveal a connection between the metabolic and redox states of monocytes and expression of the TCR-γδ ligand by demonstrating that inhibition of fatty acid or glucose utilization, or mitochondrial ROS, reduces ligand expression. Moreover, intracellular ligand expression colocalized with mitochondria. Taken together, our results expand the current understanding of the physiological

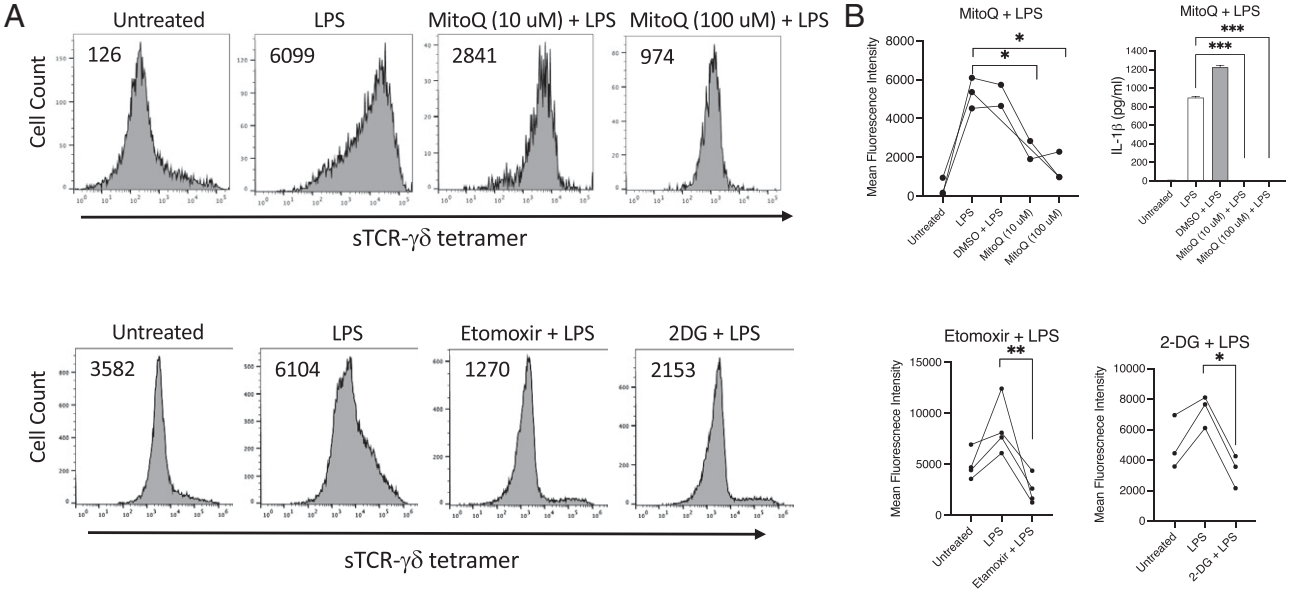

FIGURE 7. sTCR-γδ tetramer staining of activated monocytes is sensitive to inhibition of mitochondrial ROS and fatty acid and glucose utilization. LPS-activated monocytes were treated with the mitochondrial antioxidant MitoQ at the indicated concentrations, or with inhibitors of carnitine palmitoyltransferase-1, etomoxir, or glucose utilization, 2-deoxyglucose (2DG). After 48 h cells were stained with sTCR-γδ tetramer. (**A**) Representative histograms with number inserts indicating mean fluorescence intensity of entire histogram. (**B**) IL-1β levels in supernatants were determined by Luminex. Graphs summarize findings from all experiments. $*p < 0.05$, $**p < 0.005$, $***p = 0.0001$.

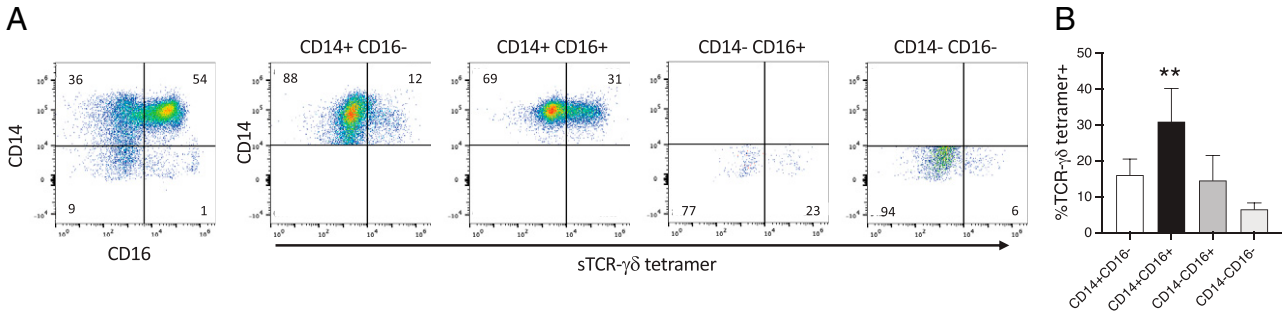

FIGURE 8. $CD14^{+}CD16^{+}$ subset of fresh monocytes expresses higher levels of TCR-γδ ligand. Freshly isolated monocytes were stained with anti-CD14, anti-CD16, and sTCR-γδ tetramer. (**A**) Shown is an example of sTCR-γδ tetramer staining of the various monocyte subsets. (**B**) Graph summarizes findings from four healthy volunteers. $^{**}p = 0.0011$.

regulation of γδ T cell ligands by defining the contributions of metabolic activity, caspases, and gasdermin-D in ligand expression.

The fact that several TLR agonists induce the TCR-γδ ligand is consistent with the known expansion of γδ T cells in response to a variety of infections, and the general benefit of γδ T cells in immune defense from numerous infections (4–10). The findings also suggested that common TLR signaling pathways might be involved with expression of the TCR-γδ ligand. This was confirmed by blocking ligand expression through inhibition of NF-κB activity as well as inhibition of various components of the caspase-dependent inflammasome. Although induction of surface ligand expression was blocked by the pan-caspase blocker zVAD, selective inhibitors of caspase-1 or caspase-8 reduced ligand expression only partially, and inhibition of caspase-3 had no effect on ligand expression. This suggested that the activity of alternate caspase or several caspases might be involved with ligand expression.

Gasdermin-D can be activated by a variety of caspases including caspase-1, caspase-4, and caspase-8 in humans, or caspase-11 in mice (40, 41, 43, 59). Similar to our findings, another study showed that LPS plus Shiga toxin 2 promoted caspase-dependent gasdermin-D activation that was independent of NLRP3 (60). Further direct targeting of gasdermin-D with a variety of inhibitors revealed its central importance in expression of the TCR-γδ ligand. Although gasdermin-D has been studied primarily for its role in cell death (40), recent work has suggested that limited gasdermin-D activation may also contribute to cellular processes other than cell death, such as the release of IL-1β (38, 39, 61, 62). Although the data in this study were intentionally gated on living cells, as defined by vital dye exclusion, it is conceivable that some of the cells were in early phases of cell death. Our findings demonstrate that gasdermin-D activation is required for export to the cell surface of the TCR-γδ ligand, or some portion of it. This may also be consistent with observations that although some TCR-γδ ligands bear MHC-like structure, as with CD1 or butyrophilins (27–30),

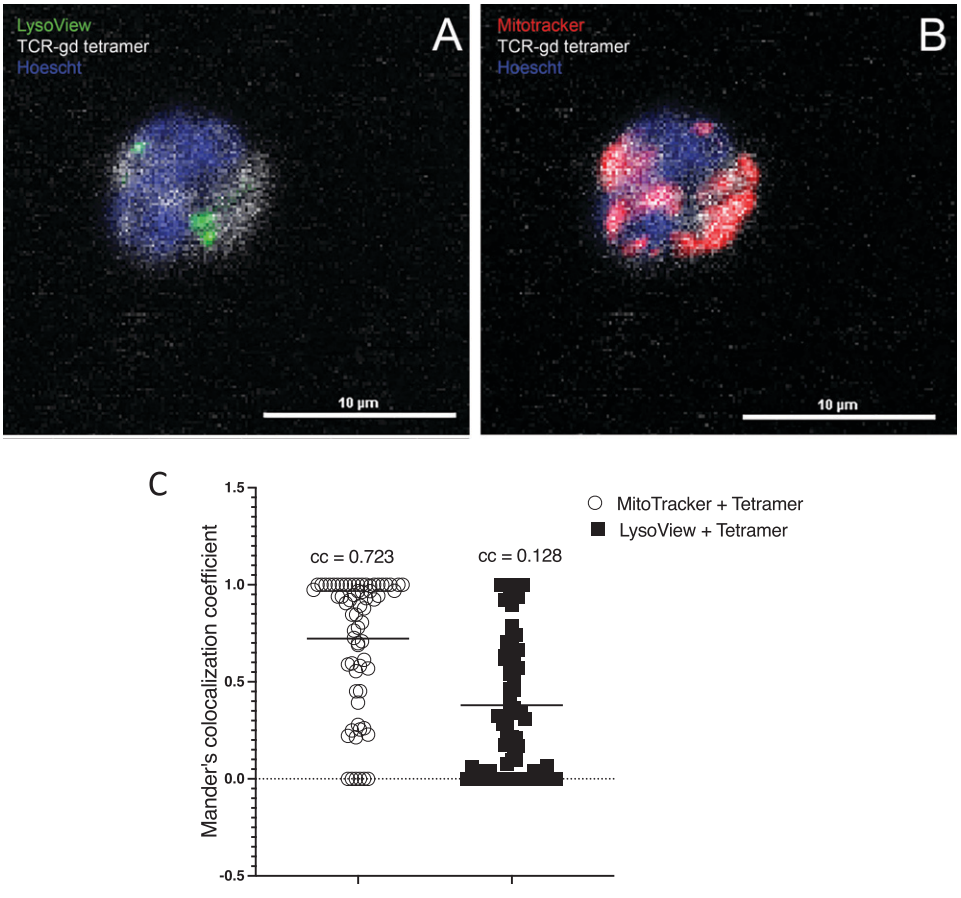

FIGURE 9. Intracellular TCR-γδ ligand colocalizes with mitochondria. (**A** and **B**) Freshly isolated monocytes were stained with LysoView (green) (A), MitoTracker (red) (B), sTCR-γδ tetramer (white), and Hoechst stain for nuclei (blue) and analyzed by confocal microscopy. Shown are representative two-dimensional images illustrating colocalization of the TCR-γδ ligand with mitochondria. (**C**) Colocalization coefficients (ccs) are shown for each of the 67 cells analyzed. Number inserts indicate the mean ccs.

they may also contain an additional component, such as sulfatide with CD1d (29).

Our study also reveals a connection between the metabolic and redox states of monocytes and the expression of the TCR-γδ ligand. Inhibition of mitochondrial ROS resulted in a corresponding decrease in the level of ligand expression. Conceivably, the TCR-γδ ligand may include an oxidized protein or lipid component, consistent with the finding that some γδ T cells recognize CD1 molecules presenting lipids, including the mitochondrial lipid cardiolipin (63). Gasdermin-D pore formation can also occur on membranes other than the plasma membrane, such as lysosomes, mitochondria, and even the nuclear membrane, promoting the release of DNA and the formation of neutrophil extracellular traps (64, 65). This property may also contribute to the release of TCR-γδ ligand components from organelles. The findings are also in agreement with a recent report demonstrating that mitochondrial ROS promote gasdermin-D oligomerization and activation (34, 35). The N-terminal fragment of gasdermin-D binds avidly to cardiolipin that is on the inner mitochondrial membrane, but it can shuttle to the outer membrane, where it could serve as a docking site for pore formation (66, 67). Gasdermin-D activation can also lead to generation of mitochondrial ROS (68, 69) and thus promote a positive feedback loop of mitochondrial ROS and gasdermin-D activation.

Confirmation of these in vitro activation studies using TLR agonists and various small molecule inhibitors comes from analysis of subsets of freshly isolated monocytes based on expression of CD14 and CD16. Compared to classical $CD14^+CD16^-$ human monocytes, the $CD14^+CD16^+$ subset manifests higher metabolic activity and ROS, increased expression of IL-1β and other inflammatory cytokines, and greater Ag presentation (56–58). That $CD14^+CD16^+$ monocytes also express considerably higher levels of surface TCR-γδ ligand than other subsets is consistent with a model of ligand expression by monocytes being dependent on active metabolism, ROS, and gasdermin-D activity. The further finding that intracellular ligand expression colocalized nearly entirely with mitochondria further underscores the notion that this TCR-γδ may recognize a self-mitochondrial component that is transported to the cell surface on metabolically active or stressed cells.

Our findings do not address the issue whether there is more than one ligand for this synovial TCR-γδ. It is entirely possible that there may be more than one ligand induced on TLR-activated monocytes that is detected by this TCR-γδ. Rather, the current study focuses on the physiological regulation of ligand expression. Multiple ligands might vary in their affinity and activation intensity for TCR-γδ and as such lead to different metabolic states of γδ T cells and functional outcomes, such as IL-17 versus IFN-γ production (70–73). In this regard, we previously used this TCR-γδ tetramer to identify a list of candidate ligands using differential tumor expression combined with RNA sequencing data and bioinformatics, as well as by mass spectrometry identification of proteins from activated monocytes that associated with the TCR-γδ (31). Among the 16 candidate ligands identified in both screens were 2 that have been previously proposed as TCR-γδ ligands, annexin A2 and Hsp70 (74–76). However, we did not observe surface induction of annexin A2 by either LPS or *Borrelia*, and only a modest induction of Hsp70 on a small subset of monocytes (Supplemental Fig. 3). Hence, it seems unlikely either molecule is the ligand observed in the current study. Moreover, as this TCR-γδ was derived from inflammatory synovium, it is noteworthy that synovial fibroblasts also express detectable surface ligand (Supplemental Fig. 4).

The current studies provide valuable information on the physiological regulation of ligand for at least one synovial Vγ9Vδ1 TCR-γδ. This adds further insight into the potential functions of γδ T cells. The role of gasdermin-D in ligand expression also underscores the prevailing view that γδ T cells monitor tissue integrity to provide immune surveillance of stressed or dying cells (3, 77) and contribute to tissue repair and wound healing (22, 23, 78–80).

Acknowledgments

We thank Dr. Roxana del Rio-Guerra for technical assistance with flow cytometry, as well as the Harry Hood Bassett Flow Cytometry and Cell Sorting Facility at the University of Vermont Larner College of Medicine. We also thank Dr. Douglas Taatjes, Nicole Bouffard, and Kyra Lee of the University of Vermont Larner College of Medicine Imaging Facility for assistance with confocal microscopy.

Disclosures

The authors have no financial conflicts of interest.

References

1. Born, W., C. Cady, J. Jones-Carson, A. Mukasa, M. Lahn, and R. O'Brien. 1999. Immunoregulatory functions of γδ T cells. *Adv. Immunol.* 71: 77–144.
2. Hayday, A. C. 2000. γδ Cells: a right time and a right place for a conserved third way of protection. *Annu. Rev. Immunol.* 18: 975–1026.
3. Kabelitz, D. 2020. Gamma delta T cells (γδ T cells) in health and disease: in memory of professor Wendy Havran. *Cells* 9: 2564.
4. Shi, C., B. Sahay, J. Q. Russell, K. A. Fortner, N. Hardin, T. J. Sellati, and R. C. Budd. 2011. Reduced immune response to *Borrelia burgdorferi* in the absence of γδ T cells. *Infect. Immun.* 79: 3940–3946.
5. Hiromatsu, K., Y. Yoshikai, G. Matsuzaki, S. Ohga, K. Muramori, K. Matsumoto, J. A. Bluestone, and K. Nomoto. 1992. A protective role of gamma/delta T cells in primary infection with *Listeria monocytogenes* in mice. *J. Exp. Med.* 175: 49–56.
6. Rosat, J. P., H. R. MacDonald, and J. A. Louis. 1993. A role for gamma delta + T cells during experimental infection of mice with *Leishmania major*. *J. Immunol.* 150: 550–555.
7. Kaufmann, S. H., and C. H. Ladel. 1994. Role of T cell subsets in immunity against intracellular bacteria: experimental infections of knock-out mice with *Listeria monocytogenes* and *Mycobacterium bovis* BCG. *Immunobiology* 191: 509–519.
8. Tsuji, M., P. Mombaerts, L. Lefrancois, R. S. Nussenzweig, F. Zavala, and S. Tonegawa. 1994. Gamma delta T cells contribute to immunity against the liver stages of malaria in alpha beta T-cell-deficient mice. *Proc. Natl. Acad. Sci. USA* 91: 345–349.
9. Mixter, P. F., V. Camerini, B. J. Stone, V. L. Miller, and M. Kronenberg. 1994. Mouse T lymphocytes that express a gamma delta T-cell antigen receptor contribute to resistance to *Salmonella* infection in vivo. *Infect. Immun.* 62: 4618–4621.
10. Costa, G., S. Loizon, M. Guenot, I. Mocan, F. Halary, G. de Saint-Basile, V. Pitard, J. Déchanet-Merville, J. F. Moreau, M. Troye-Blomberg, et al. 2011. Control of *Plasmodium falciparum* erythrocytic cycle: γδ T cells target the red blood cell-invasive merozoites. *Blood* 118: 6952–6962.
11. Zhao, Y., C. Niu, and J. Cui. 2018. Gamma-delta (γδ) T cells: friend or foe in cancer development? [Published erratum appears in 2018 *J. Transl. Med.* 16: 122.] *J. Transl. Med.* 16: 3 .
12. Girardi, M., D. E. Oppenheim, C. R. Steele, J. M. Lewis, E. Glusac, R. Filler, P. Hobby, B. Sutton, R. E. Tigelaar, and A. C. Hayday. 2001. Regulation of cutaneous malignancy by γδ T cells. *Science* 294: 605–609.
13. Brennan, F. M., M. Londei, A. M. Jackson, T. Hercend, M. B. Brenner, R. N. Maini, and M. Feldmann. 1988. T cells expressing gamma delta chain receptors in rheumatoid arthritis. *J. Autoimmun.* 1: 319–326.
14. Vincent, M. S., K. Roessner, D. Lynch, D. Wilson, S. M. Cooper, J. Tschopp, L. H. Sigal, and R. C. Budd. 1996. Apoptosis of Fas^{high} $CD4^+$ synovial T cells by *Borrelia*-reactive Fas-$ligand^{high}$ γδ T cells in Lyme arthritis. *J. Exp. Med.* 184: 2109–2117.
15. Rust, C., Y. Kooy, S. Peña, M. L. Mearin, P. Kluin, and F. Koning. 1992. Phenotypical and functional characterization of small intestinal TcRγδ$^+$ T cells in coeliac disease. *Scand. J. Immunol.* 35: 459–468.
16. Balbi, B., D. R. Moller, M. Kirby, K. J. Holroyd, and R. G. Crystal. 1990. Increased numbers of T lymphocytes with gamma delta-positive antigen receptors in a subgroup of individuals with pulmonary sarcoidosis. *J. Clin. Invest.* 85: 1353–1361.
17. Peterman, G. M., C. Spencer, A. I. Sperling, and J. A. Bluestone. 1993. Role of gamma delta T cells in murine collagen-induced arthritis. *J. Immunol.* 151: 6546–6558.
18. Pelegrí, C., P. Kühnlein, E. Buchner, C. B. Schmidt, A. Franch, M. Castell, T. Hünig, F. Emmrich, and R. W. Kinne. 1996. Depletion of γ/δ T cells does not prevent or ameliorate, but rather aggravates, rat adjuvant arthritis. *Arthritis Rheum.* 39: 204–215.
19. Peng, S. L., M. P. Madaio, A. C. Hayday, and J. Craft. 1996. Propagation and regulation of systemic autoimmunity by gammadelta T cells. *J. Immunol.* 157: 5689–5698.
20. Mukasa, A., K. Hiromatsu, G. Matsuzaki, R. O'Brien, W. Born, and K. Nomoto. 1995. Bacterial infection of the testis leading to autoaggressive immunity triggers apparently opposed responses of alpha beta and gamma delta T cells. *J. Immunol.* 155: 2047–2056.

21. Witherden, D. A., K. Ramirez, and W. L. Havran. 2014. Multiple receptor-ligand interactions direct tissue-resident γδ T cell activation. *Front. Immunol.* 5: 602.
22. Nielsen, M. M., D. A. Witherden, and W. L. Havran. 2017. γδ T cells in homeostasis and host defence of epithelial barrier tissues. *Nat. Rev. Immunol.* 17: 733–745.
23. Komori, H. K., D. A. Witherden, R. Kelly, K. Sendaydiego, J. M. Jameson, L. Teyton, and W. L. Havran. 2012. Cutting edge: dendritic epidermal γδ T cell ligands are rapidly and locally expressed by keratinocytes following cutaneous wounding. *J. Immunol.* 188: 2972–2976.
24. Kohlgruber, A. C., S. T. Gal-Oz, N. M. LaMarche, M. Shimazaki, D. Duquette, H. F. Koay, H. N. Nguyen, A. I. Mina, T. Paras, A. Tavakkoli, et al. 2018. γδ T cells producing interleukin-17A regulate adipose regulatory T cell homeostasis and thermogenesis. [Published erratum appears in 2019 *Nat. Immunol.* 20: 373.] *Nat. Immunol.* 19: 464–474.
25. Vincent, M. S., K. Roessner, T. Sellati, C. D. Huston, L. H. Sigal, S. M. Behar, J. D. Radolf, and R. C. Budd. 1998. Lyme arthritis synovial γδ T cells respond to *Borrelia burgdorferi* lipoproteins and lipidated hexapeptides. *J. Immunol.* 161: 5762–5771.
26. Constant, P., F. Davodeau, M. A. Peyrat, Y. Poquet, G. Puzo, M. Bonneville, and J. J. Fournié. 1994. Stimulation of human γδ T cells by nonpeptidic mycobacterial ligands. *Science* 264: 267–270.
27. Harly, C., Y. Guillaume, S. Nedellec, C. M. Peigné, H. Mönkkönen, J. Mönkkönen, J. Li, J. Kuball, E. J. Adams, S. Netzer, et al. 2012. Key implication of CD277/butyrophilin-3 (BTN3A) in cellular stress sensing by a major human γδ T-cell subset. *Blood* 120: 2269–2279.
28. Rigau, M., S. Ostrouska, T. S. Fulford, D. N. Johnson, K. Woods, Z. Ruan, H. E. G. McWilliam, C. Hudson, C. Tutuka, A. K. Wheatley, et al. 2020. Butyrophilin 2A1 is essential for phosphoantigen reactivity by γδ T cells. *Science* 367: eaay5516.
29. Luoma, A. M., C. D. Castro, T. Mayassi, L. A. Bembinster, L. Bai, D. Picard, B. Anderson, L. Scharf, J. E. Kung, L. V. Sibener, et al. 2013. Crystal structure of Vδ1 T cell receptor in complex with CD1d-sulfatide shows MHC-like recognition of a self-lipid by human γδ T cells. *Immunity* 39: 1032–1042.
30. Roy, S., D. Ly, C. D. Castro, N. S. Li, A. J. Hawk, J. D. Altman, S. C. Meredith, J. A. Piccirilli, D. B. Moody, and E. J. Adams. 2016. Molecular analysis of lipid-reactive Vδ1 γδ T cells identified by CD1c tetramers. *J. Immunol.* 196: 1933–1942.
31. Collins, C., Y. Lui, A. M. Santos, B. A. Ballif, A. M. Gogerly-Moragoda, H. Brouwer, R. Ross, K. Balagurunathan, S. Sharma, G. J. Wright, et al. 2019. Detection of cell surface ligands for human synovial γδ T cells. *J. Immunol.* 203: 2369–2376.
32. Collins, C., C. Shi, J. Q. Russell, K. A. Fortner, and R. C. Budd. 2008. Activation of γδ T cells by *Borrelia burgdorferi* is indirect via a TLR- and caspase-dependent pathway. *J. Immunol.* 181: 2392–2398.
33. Hirschfeld, M., C. J. Kirschning, R. Schwandner, H. Wesche, J. H. Weis, R. M. Wooten, and J. J. Weis. 1999. Cutting edge: inflammatory signaling by *Borrelia burgdorferi* lipoproteins is mediated by Toll-like receptor 2. *J. Immunol.* 163: 2382–2386.
34. Wang, Y., P. Shi, Q. Chen, Z. Huang, D. Zou, J. Zhang, X. Gao, and Z. Lin. 2019. Mitochondrial ROS promote macrophage pyroptosis by inducing GSDMD oxidation. *J. Mol. Cell Biol.* 11: 1069–1082.
35. Evavold, C. L., I. Hafner-Bratkovič, P. Devant, J. M. D'Andrea, E. M. Ngwa, E. Boršić, J. G. Doench, M. W. LaFleur, A. H. Sharpe, J. R. Thiagarajah, and J. C. Kagan. 2021. Control of gasdermin D oligomerization and pyroptosis by the Ragulator-Rag-mTORC1 pathway. *Cell* 184: 4495–4511.e19.
36. Kappler, J., J. White, H. Kozono, J. Clements, and P. Marrack. 1994. Binding of a soluble alpha beta T-cell receptor to superantigen/major histocompatibility complex ligands. *Proc. Natl. Acad. Sci. USA* 91: 8462–8466.
37. Aydintug, M. K., C. L. Roark, X. Yin, J. M. Wands, W. K. Born, and R. L. O'Brien. 2004. Detection of cell surface ligands for the γδ TCR using soluble TCRs. *J. Immunol.* 172: 4167–4175.
38. Gaidt, M. M., T. S. Ebert, D. Chauhan, T. Schmidt, J. L. Schmid-Burgk, F. Rapino, A. A. Robertson, M. A. Cooper, T. Graf, and V. Hornung. 2016. Human monocytes engage an alternative inflammasome pathway. *Immunity* 44: 833–846.
39. Evavold, C. L., J. Ruan, Y. Tan, S. Xia, H. Wu, and J. C. Kagan. 2018. the pore-forming protein gasdermin D regulates interleukin-1 secretion from living macrophages. *Immunity* 48: 35–44.e6.
40. Kayagaki, N., I. B. Stowe, B. L. Lee, K. O'Rourke, K. Anderson, S. Warming, T. Cuellar, B. Haley, M. Roose-Girma, Q. T. Phung, et al. 2015. Caspase-11 cleaves gasdermin D for non-canonical inflammasome signalling. *Nature* 526: 666–671.
41. Liu, Z., C. Wang, J. Yang, Y. Chen, B. Zhou, D. W. Abbott, and T. S. Xiao. 2020. Caspase-1 engages full-length gasdermin D through two distinct interfaces that mediate caspase recruitment and substrate cleavage. *Immunity* 53: 106–114.e5.
42. Shi, J., Y. Zhao, K. Wang, X. Shi, Y. Wang, H. Huang, Y. Zhuang, T. Cai, F. Wang, and F. Shao. 2015. Cleavage of GSDMD by inflammatory caspases determines pyroptotic cell death. *Nature* 526: 660–665.
43. Yang, J., Z. Liu, C. Wang, R. Yang, J. K. Rathkey, O. W. Pinkard, W. Shi, Y. Chen, G. R. Dubyak, D. W. Abbott, and T. S. Xiao. 2018. Mechanism of gasdermin D recognition by inflammatory caspases and their inhibition by a gasdermin D-derived peptide inhibitor. *Proc. Natl. Acad. Sci. USA* 115: 6792–6797.
44. Humphries, F., L. Shmuel-Galia, N. Ketelut-Carneiro, S. Li, B. Wang, V. V. Nemmara, R. Wilson, Z. Jiang, F. Khalighinejad, K. Muneeruddin, et al. 2020. Succination inactivates gasdermin D and blocks pyroptosis. *Science* 369: 1633–1637.
45. Rathkey, J. K., J. Zhao, Z. Liu, Y. Chen, J. Yang, H. C. Kondolf, B. L. Benson, S. M. Chirieleison, A. Y. Huang, G. R. Dubyak, et al. 2018. Chemical disruption of the pyroptotic pore-forming protein gasdermin D inhibits inflammatory cell death and sepsis. *Sci. Immunol.* 3: eaat2738.
46. Liao, D., L. Sun, H. Sudan, X. Wang, and X. Lei. 2014. Necrosulfonamide inhibits necroptosis by selectively targeting the mixed lineage kinase domain-like protein. *MedChemComm* 5: 333–337.
47. Degterev, A., J. Hitomi, M. Germscheid, I. L. Ch'en, O. Korkina, X. Teng, D. Abbott, G. D. Cuny, C. Yuan, G. Wagner, et al. 2008. Identification of RIP1 kinase as a specific cellular target of necrostatins. *Nat. Chem. Biol.* 4: 313–321.
48. Yamada, H., T. Arai, N. Endo, K. Yamashita, K. Fukuda, M. Sasada, and T. Uchiyama. 2006. LPS-induced ROS generation and changes in glutathione level and their relation to the maturation of human monocyte-derived dendritic cells. *Life Sci.* 78: 926–933.
49. Thwe, P. M., and E. Amiel. 2018. The role of nitric oxide in metabolic regulation of dendritic cell immune function. *Cancer Lett.* 412: 236–242.
50. Adlam, V. J., J. C. Harrison, C. M. Porteous, A. M. James, R. A. Smith, M. P. Murphy, and I. A. Sammut. 2005. Targeting an antioxidant to mitochondria decreases cardiac ischemia-reperfusion injury. *FASEB J.* 19: 1088–1095.
51. Gane, E. J., F. Weilert, D. W. Orr, G. F. Keogh, M. Gibson, M. M. Lockhart, C. M. Frampton, K. M. Taylor, R. A. Smith, and M. P. Murphy. 2010. The mitochondria-targeted anti-oxidant mitoquinone decreases liver damage in a phase II study of hepatitis C patients. *Liver Int.* 30: 1019–1026.
52. Murphy, M. P. 2016. Understanding and preventing mitochondrial oxidative damage. *Biochem. Soc. Trans.* 44: 1219–1226.
53. Declercq, P. E., J. R. Falck, M. Kuwajima, H. Tyminski, D. W. Foster, and J. D. McGarry. 1987. Characterization of the mitochondrial carnitine palmitoyltransferase enzyme system. I. Use of inhibitors. *J. Biol. Chem.* 262: 9812–9821.
54. Everts, B., E. Amiel, G. J. van der Windt, T. C. Freitas, R. Chott, K. E. Yarasheski, E. L. Pearce, and E. J. Pearce. 2012. Commitment to glycolysis sustains survival of NO-producing inflammatory dendritic cells. *Blood* 120: 1422–1431.
55. Pelicano, H., D. S. Martin, R. H. Xu, and P. Huang. 2006. Glycolysis inhibition for anticancer treatment. *Oncogene* 25: 4633–4646.
56. Ziegler-Heitbrock, L. 2007. The $CD14^+$ $CD16^+$ blood monocytes: their role in infection and inflammation. *J. Leukoc. Biol.* 81: 584–592.
57. Ancuta, P., K. Y. Liu, V. Misra, V. S. Wacleche, A. Gosselin, X. Zhou, and D. Gabuzda. 2009. Transcriptional profiling reveals developmental relationship and distinct biological functions of $CD16^+$ and $CD16^-$ monocyte subsets. *BMC Genomics* 10: 403.
58. Stansfield, B. K., and D. A. Ingram. 2015. Clinical significance of monocyte heterogeneity. *Clin. Transl. Med.* 4: 5.
59. Liu, Z., B. M. Busscher, M. Storl-Desmond, and T. S. Xiao. 2022. Mechanisms of gasdermin recognition by proteases. *J. Mol. Biol.* 434: 167274.
60. Platnich, J. M., H. Chung, A. Lau, C. F. Sandall, A. Bondzi-Simpson, H. M. Chen, T. Komada, A. C. Trotman-Grant, J. R. Brandelli, J. Chun, et al. 2018. Shiga toxin/lipopolysaccharide activates caspase-4 and gasdermin D to trigger mitochondrial reactive oxygen species upstream of the NLRP3 inflammasome. *Cell Rep.* 25: 1525–1536.e7.
61. Chen, K. W., C. J. Groß, F. V. Sotomayor, K. J. Stacey, J. Tschopp, M. J. Sweet, and K. Schroder. 2014. The neutrophil NLRC4 inflammasome selectively promotes IL-1β maturation without pyroptosis during acute *Salmonella* challenge. *Cell Rep.* 8: 570–582.
62. Zanoni, I., Y. Tan, M. Di Gioia, A. Broggi, J. Ruan, J. Shi, C. A. Donado, F. Shao, H. Wu, J. R. Springstead, and J. C. Kagan. 2016. An endogenous caspase-11 ligand elicits interleukin-1 release from living dendritic cells. *Science* 352: 1232–1236.
63. Dieudé, M., H. Striegl, A. J. Tyznik, J. Wang, S. M. Behar, C. A. Piccirillo, J. S. Levine, D. M. Zajonc, and J. Rauch. 2011. Cardiolipin binds to CD1d and stimulates CD1d-restricted γδ T cells in the normal murine repertoire. *J. Immunol.* 186: 4771–4781.
64. Sollberger, G., A. Choidas, G. L. Burn, P. Habenberger, R. Di Lucrezia, S. Kordes, S. Menninger, J. Eickhoff, P. Nussbaumer, B. Klebl, et al. 2018. Gasdermin D plays a vital role in the generation of neutrophil extracellular traps. *Sci. Immunol.* 3: eaar6689.
65. Chen, K. W., M. Monteleone, D. Boucher, G. Sollberger, D. Ramnath, N. D. Condon, J. B. von Pein, P. Broz, M. J. Sweet, and K. Schroder. 2018. Noncanonical inflammasome signaling elicits gasdermin D-dependent neutrophil extracellular traps. *Sci. Immunol.* 3: eaar6676.
66. Ding, J., K. Wang, W. Liu, Y. She, Q. Sun, J. Shi, H. Sun, D. C. Wang, and F. Shao. 2016. Pore-forming activity and structural autoinhibition of the gasdermin family. [Published erratum appears in 2016 *Nature* 540: 150.] *Nature* 535: 111–116.
67. Liu, X., Z. Zhang, J. Ruan, Y. Pan, V. G. Magupalli, H. Wu, and J. Lieberman. 2016. Inflammasome-activated gasdermin D causes pyroptosis by forming membrane pores. *Nature* 535: 153–158.
68. Rogers, C., D. A. Erkes, A. Nardone, A. E. Aplin, T. Fernandes-Alnemri, and E. S. Alnemri. 2019. Gasdermin pores permeabilize mitochondria to augment caspase-3 activation during apoptosis and inflammasome activation. *Nat. Commun.* 10: 1689.
69. Lieberman, J., H. Wu, and J. C. Kagan. 2019. Gasdermin D activity in inflammation and host defense. *Sci. Immunol.* 4: eaav1447.
70. Wu, P., D. Wu, C. Ni, J. Ye, W. Chen, G. Hu, Z. Wang, C. Wang, Z. Zhang, W. Xia, et al. 2014. γδT17 cells promote the accumulation and expansion of myeloid-derived suppressor cells in human colorectal cancer. *Immunity* 40: 785–800.
71. Coffelt, S. B., K. Kersten, C. W. Doornebal, J. Weiden, K. Vrijland, C. S. Hau, N. J. M. Verstegen, M. Ciampricotti, L. J. A. C. Hawinkels, J. Jonkers, and K. E. de Visser. 2015. IL-17-producing γδ T cells and neutrophils conspire to promote breast cancer metastasis. *Nature* 522: 345–348.
72. Melandri, D., I. Zlatareva, R. A. G. Chaleil, R. J. Dart, A. Chancellor, O. Nussbaumer, O. Polyakova, N. A. Roberts, D. Wesch, D. Kabelitz, et al. 2018. The γδTCR combines innate immunity with adaptive immunity by utilizing spatially distinct regions for agonist selection and antigen responsiveness. *Nat. Immunol.* 19: 1352–1365.
73. Reis, B. S., P. W. Darcy, I. Z. Khan, C. S. Moon, A. E. Kornberg, V. S. Schneider, Y. Alvarez, O. Eleso, C. Zhu, M. Schernthanner, et al. 2022. TCR-Vγδ usage distinguishes protumor from antitumor intestinal γδ T cell subsets. *Science* 377: 276–284.

74. Marlin, R., A. Pappalardo, H. Kaminski, C. R. Willcox, V. Pitard, S. Netzer, C. Khairallah, A. M. Lomenech, C. Harly, M. Bonneville, et al. 2017. Sensing of cell stress by human γδ TCR-dependent recognition of annexin A2. *Proc. Natl. Acad. Sci. USA* 114: 3163–3168.
75. Born, W., L. Hall, A. Dallas, J. Boymel, T. Shinnick, D. Young, P. Brennan, and R. O'Brien. 1990. Recognition of a peptide antigen by heat shock–reactive γδ T lymphocytes. *Science* 249: 67–69.
76. Chen, H., X. He, Z. Wang, D. Wu, H. Zhang, C. Xu, H. He, L. Cui, D. Ba, and W. He. 2008. Identification of human T cell receptor γδ-recognized epitopes/proteins via CDR3δ peptide-based immunobiochemical strategy. *J. Biol. Chem.* 283: 12528–12537.
77. Hayday, A. C. 2019. γδ T cell update: adaptate orchestrators of immune surveillance. *J. Immunol.* 203: 311–320.
78. Havran, W. L., Y. H. Chien, and J. P. Allison. 1991. Recognition of self antigens by skin-derived T cells with invariant γδ antigen receptors. *Science* 252: 1430–1432.
79. Witherden, D. A., M. Watanabe, O. Garijo, S. E. Rieder, G. Sarkisyan, S. J. Cronin, P. Verdino, I. A. Wilson, A. Kumanogoh, H. Kikutani, et al. 2012. The CD100 receptor interacts with its plexin B2 ligand to regulate epidermal γδ T cell function. *Immunity* 37: 314–325.
80. Johnson, M. D., D. A. Witherden, and W. L. Havran. 2020. The role of tissue-resident γδ T cells in stress surveillance and tissue maintenance. *Cells* 9: 686–704.